Interrupted Pressure-Jump NMR Experiments Reveal Resonances of On-Pathway Protein Folding Intermediate

*Cyril Charlier‡, Joseph M. Courtney‡, Philip Anfinrud, and Ad Bax**

Laboratory of Chemical Physics, NIDDK, National Institutes of Health, Bethesda, MD, 20892-0520, USA

SUPPORTING INFORMATION

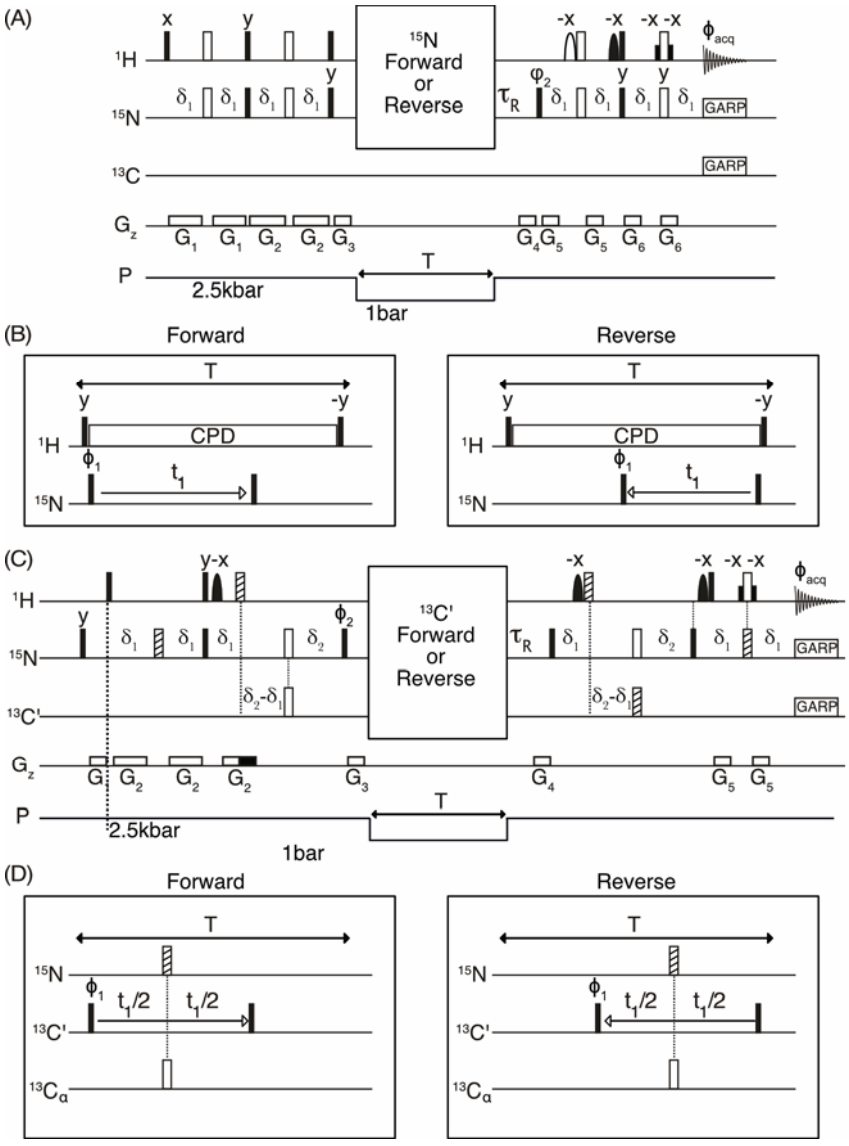

Figure S1. Pressure-jump 2D pulse schemes for correlating the ^{15}N and ^{13}C′ chemical shifts of the unfolded, intermediate, and folded states at 1 bar, to $^{1}H^{N}$ shifts at high pressure. The magnetization is transferred from ^{1}H to (A) ^{15}N or (C) ^{13}C′ at 2.5 kbar and then the pressure is dropped to 1 bar, prior to t_1 evolution of (A,B) the ^{15}N or (C,D) ^{13}C′ frequency. Evolution of transverse (B) ^{15}N or (D) ^{13}C′ is encoded by a $90°_{\phi 1} - t_1 - 90°_{x}$ pulse pair, with the first pulse applied immediately after the pressure-drop is completed (Forward sampling) or with the second pulse applied just prior to the switch back to high pressure (Reverse sampling). In both cases, the second 90° stores a cosine- (or sine-)modulated fraction of the ^{15}N or ^{13}C′ magnetization along *z*, with residual transverse magnetization destroyed by gradient G_4. After the pressure is jumped back to 2.5kbar, the t_1-encoded *z* magnetization is transferred back to ^{1}H for detection. Filled and open symbols on the ^{1}H and ^{15}N radiofrequency channels represent 90° and 180° pulses, respectively. Shaped pulses are selectively applied to the water resonance, as are the weak rectangular 90° pulses that are part of the standard WATERGATE element.[1] Unless indicated, pulse phases are *x*. Data were recorded with $\phi_1 = \{x, -x\}$, $\phi_2 = \{x, x, -x, -x\}$, $\phi_{acq} = \{x, -x, -x, x\}$; Hatched rectangles indicate $90°_{x}$-$210°_{y}$-$90°_{x}$ composite pulses.[2] The INEPT delays are $\delta_1 = 2.56$ ms and $\delta_2 = 15.3$ ms. The maximum t_1 evolution time is 60 ms and the total low-pressure period is 70 ms. Pulsed field gradients are either sine-bell shaped

($G_{3,4}$) or weak, rectangular ($G_{1,2,4,5}$). ^{1}H decoupling during ^{15}N evolution (labeled CPD) uses the WALTZ16 modulation scheme, remains on during the full low-pressure period, and is bracketed by 90° pulses to return the water magnetization parallel to the CPD radiofrequency field and back to the *z* axis. Short (5 ms) "padding" delays separate the midpoints of the pressure jumps from application of the first (for forward sampling) or last (for reverse sampling) 90° pulses that initiate and terminate the t_1 evolution period, thereby ensuring that the slower tail of the pressure jump does not impact evolution, and to accommodate potential fluctuations in the mechanical valve timing. The recovery delay, τ_R (~150 ms), serves to let die down any vibrations and sample flow which can have adverse effects on ^{1}H signal detection and rephasing by pulsed field gradients.

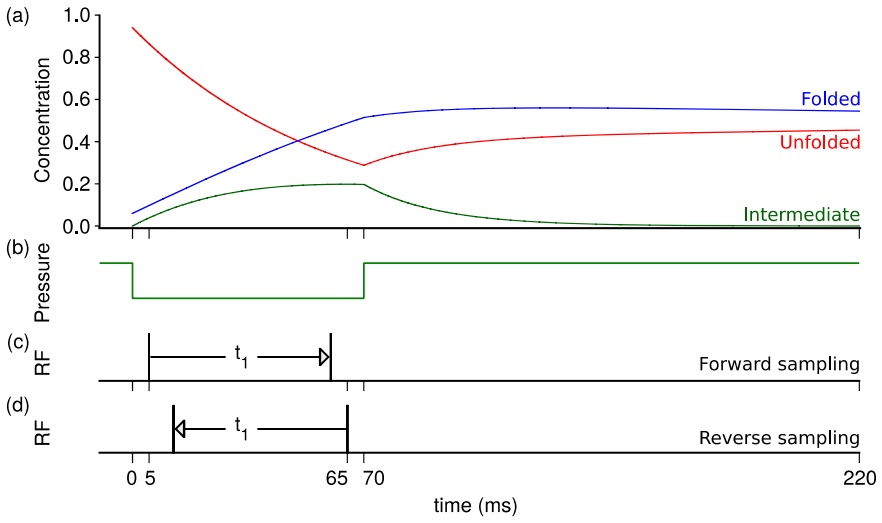

Figure S2. Evolution of the concentration of the unfolded, intermediate, and folded species in a pressure-jump experiment of the type shown in Figure 1, main text. (A) Concentration as a function of time: folded (blue), unfolded (red) and intermediate (green) obtained by the integration of a 3-state rate equation (Eq SI.1) where [U](t), [F](t) and [I](t) are the respective concentrations, and k are the rate constants for the different transitions.

$$\frac{d}{dt}\begin{bmatrix}[\mathrm{U}](t)\\ [\mathrm{I}](t)\\ [\mathrm{F}](t)\end{bmatrix} = \begin{bmatrix}-(k_{U\to I}+k_{U\to F}) & k_{I\to U} & k_{F\to U}\\ k_{U\to I} & -(k_{I\to U}+k_{I\to F}) & k_{F\to I}\\ k_{U\to F} & k_{I\to F} & -(k_{F\to U}+k_{F\to I})\end{bmatrix}\begin{bmatrix}[\mathrm{U}](t)\\ [\mathrm{I}](t)\\ [\mathrm{F}](t)\end{bmatrix} \qquad \text{(SI.1)}$$

After the initial high-pressure period (~8s), 94% of the protein is in the unfolded states (t = 0). During the low-pressure period the previously derived rate constants[3] are $k_{U\to F} = 8\ s^{-1}, k_{U\to I} = 8.9\ s^{-1}, k_{I\to F} = 14.2\ s^{-1}$ with all other rates zero. During the high-pressure period, the rates used for the simulation are $k_{F\to U} = 0.4\ s^{-1}, k_{I\to U} = 30\ s^{-1}, k_{I\to F} = 14.2\ s^{-1}$, with all other rates set to zero. Note that no experimental values for $k_{I\to U}$ and $k_{I\to F}$ at high pressure were measured, but their ratio is approximately two based on peak intensity ratios, and the sum of their rates is ≥30 s^{-1}. The t_1 evolution period is padded at either end by 5-ms delays to minimize the effect of small experimental jitter in the valve opening and closing times, and allow for pressure equilibration which switches to slow, laminar flow when the sample cell approaches its target pressure.

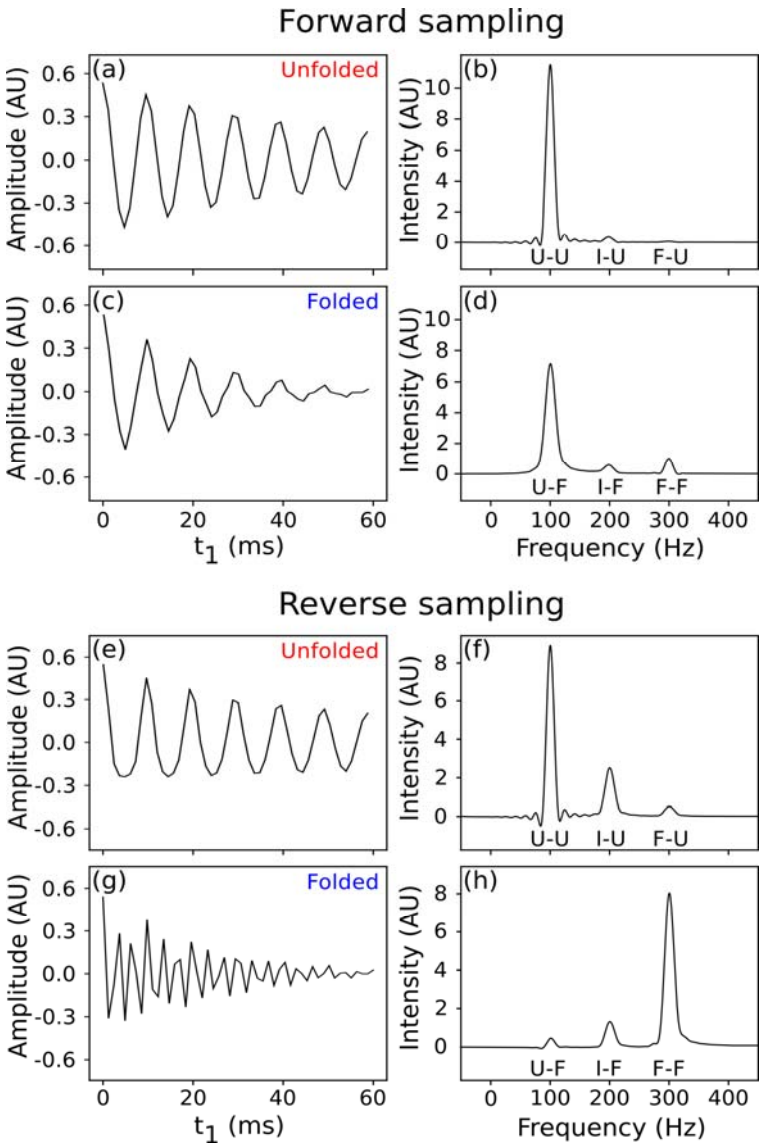

Figure S3. Simulation of forward and reverse sampled NMR data with the pulse scheme of Figure S1A,B, using the populations of the U, I, and F states shown in Figure S2. Simulated interferograms (t_1 dimension; left column) corresponding to t_1-modulated magnetization of the unfolded (A,E) and folded (C,G) species just before transfer to ^{1}H for detection (i.e. the end of the time course shown in figure S2). Fourier transformed interferograms (right column) for the species that are unfolded (B,F) and folded (D,H) during the high-pressure ^{1}H detection period. The concentration of the intermediate species is negligible at this point and is therefore not shown. The folded, I, and F species are set to frequencies of 100, 200, and 300 Hz, respectively. The pulse sequence with pressure jumps depicted in Figure S2 was simulated by integrating the Bloch-McConnell equation for non-equilibrium reactions.[4] The simulation began with *Z* magnetization of all three species at equilibrium concentrations. The second pulse in each scan was phase cycled to rotate either the *X*- or *Y*-component of the magnetization back to the *Z*-axis and to suppress axial peaks. At the end of each scan, the signal was "detected" by extracting the *Z* component of the magnetization for each species. The resulting FIDs for each of the species were then apodized with a cosine bell, zero-filled, and Fourier transformed. Note that the very weak I-U, I-F and F-F signals in the forward sampled spectra result from processes during the 5-ms "padding delay" that precedes t_1.

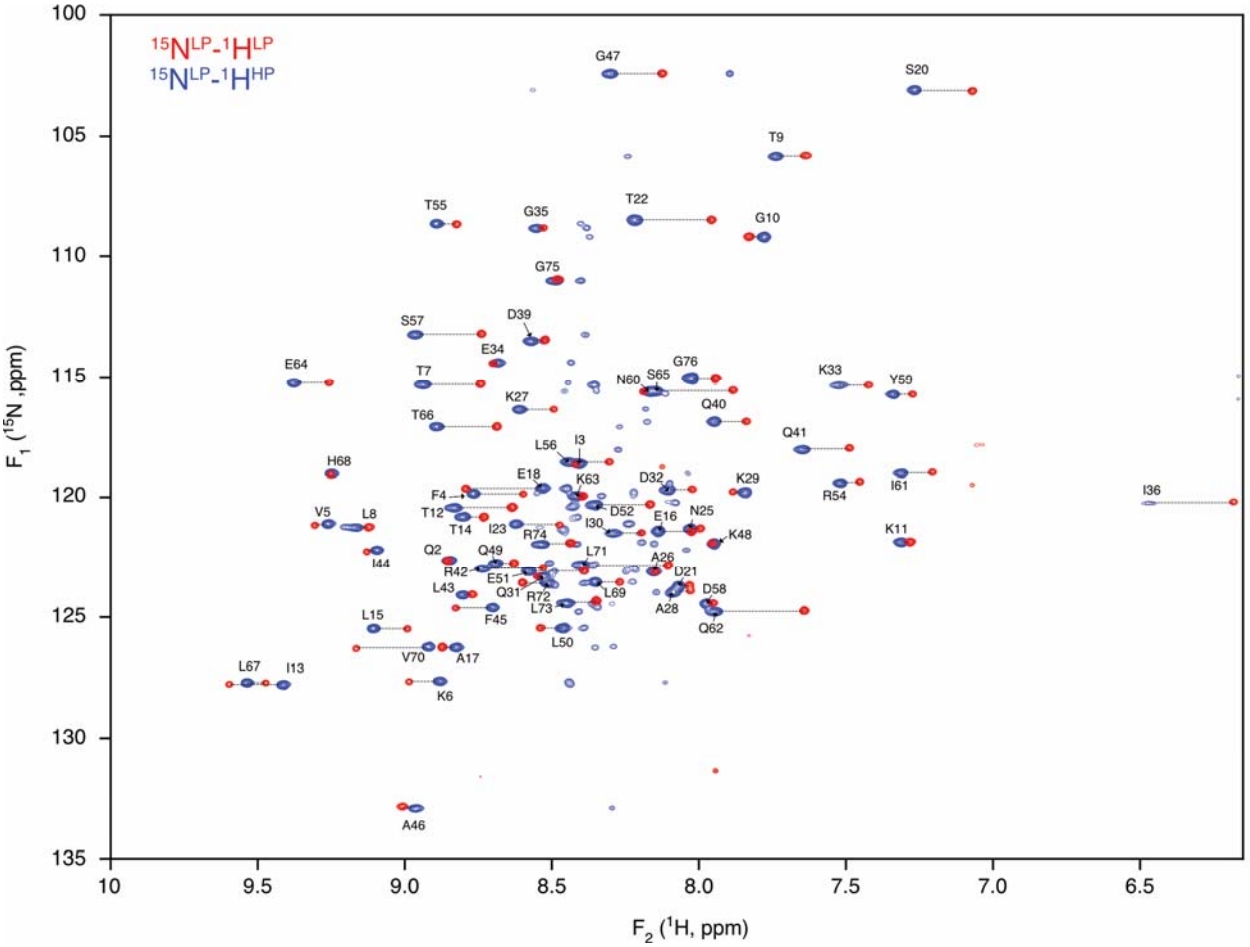

Figure S4. Pressure-jump HSQC spectrum (blue contours, labeled by residue type and number) of VA2-ubiquitin, recorded at 600 MHz, pH 6.4, with the temperature regulated at 22 °C during the long (9 s) low pressure equilibration and t_1 evolution delay, superimposed on a regular, 1-bar HSQC spectrum (red contours). Weak, unlabeled blue peaks correspond to proteins that unfolded during the ~150-ms vibration recovery delay, prior to detection of the ^{1}H signals, appearing at the folded ^{15}N frequency at 1 bar correlated to unfolded protein $^1H^N$ frequency at 2.5 kbar. The spectrum was recorded with the forward scheme of Figure S1A, but the pressure kept low during the preparation interval, and only switched to high (2.5 kbar) from the end of t_1 evolution until the end of ^{1}H data acquisition. The spectrum was recorded with 4 scans per complex t_1 increment, for a total duration of 2.5 h.

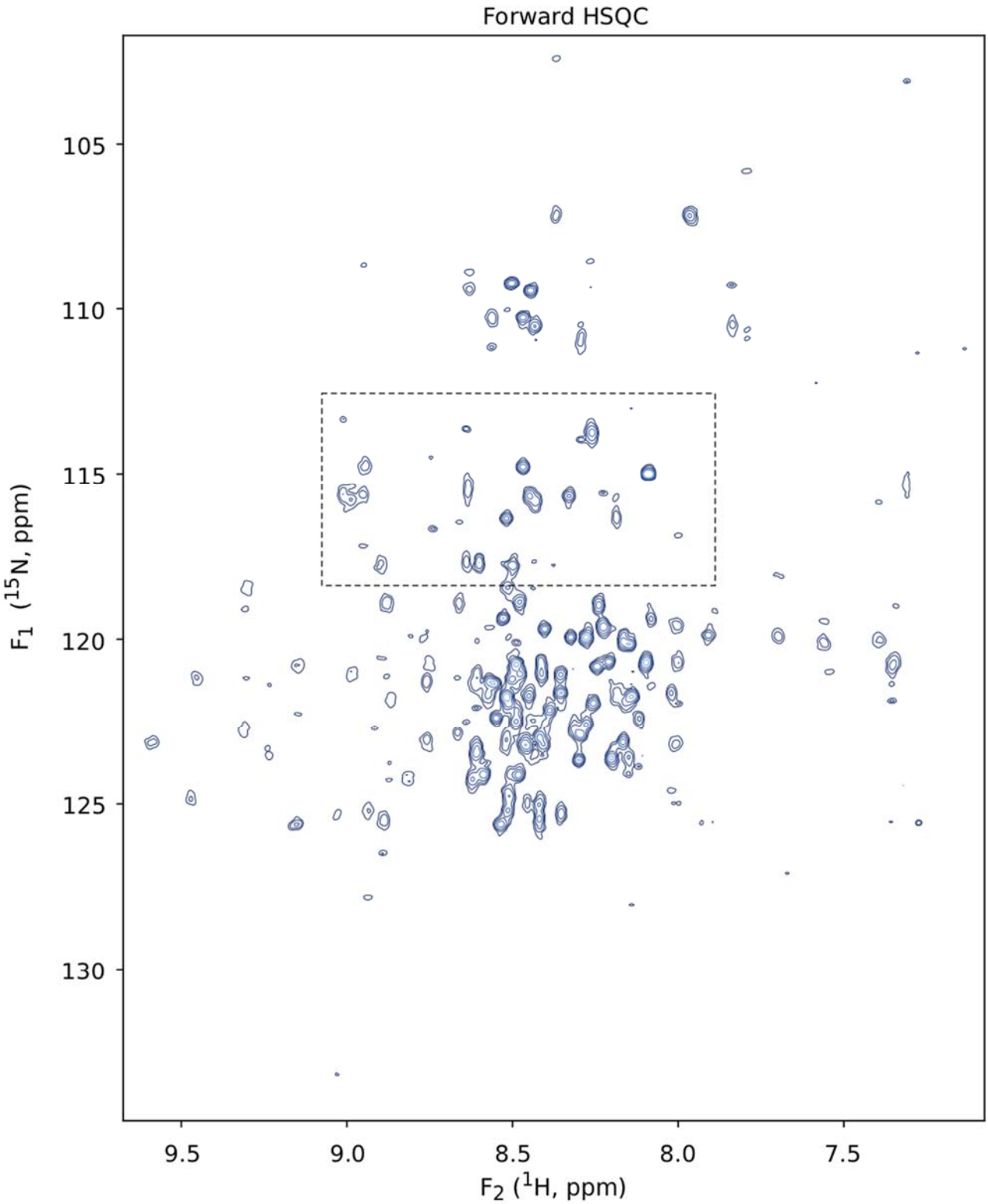

Figure S5. Pressure-jump forward-sampled 2D ^{1}H-^{15}N HSQC spectrum of VA2-ubiquitin, with the boxed region shown in Figure 2, main text.

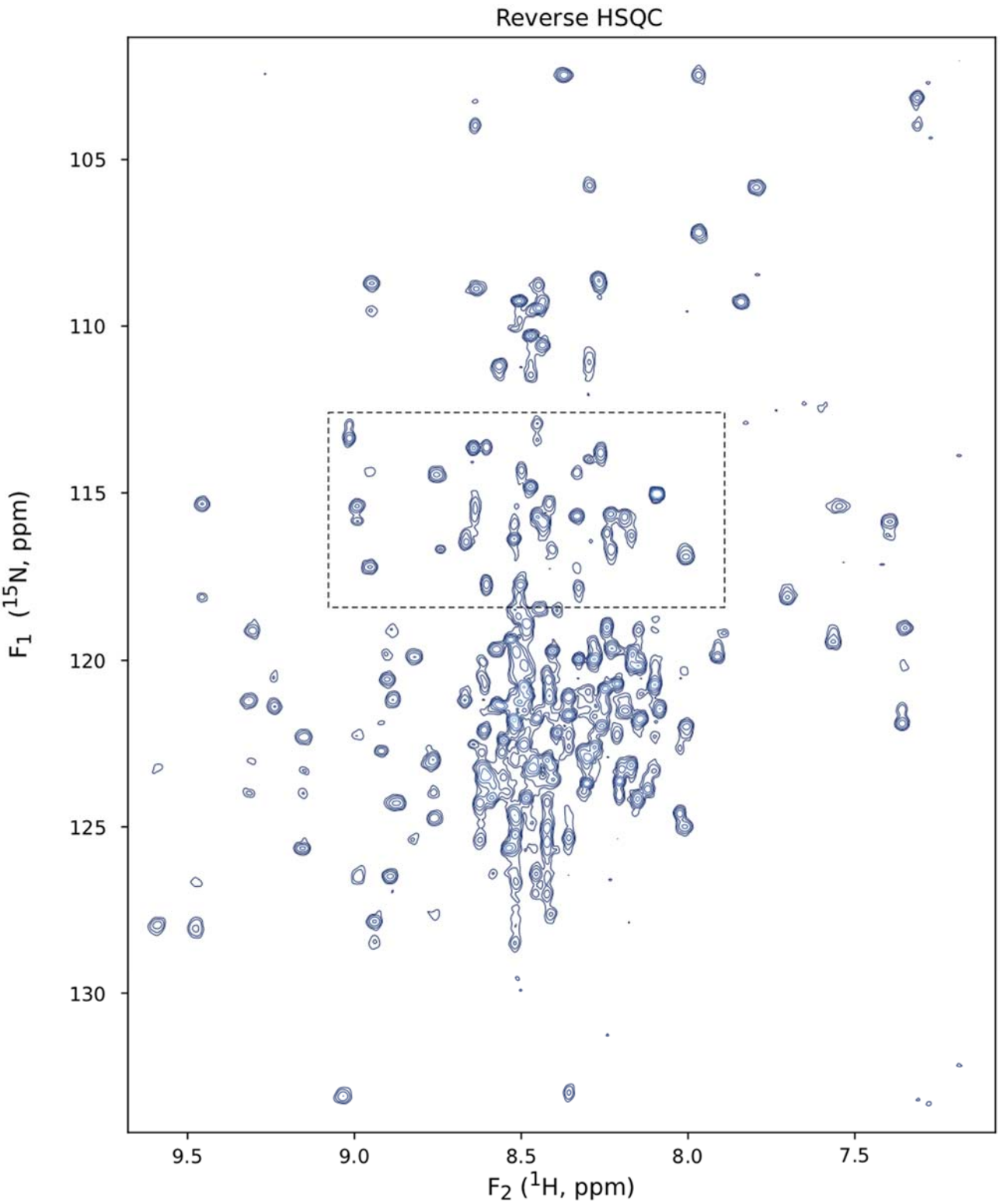

Figure S6. Pressure-jump reverse-sampled 2D ^{1}H-^{15}N HSQC spectrum of VA2-ubiquitin with the boxed region shown in Figure 2, main text. Peak positions of the I-state correspond to those of Table S1.

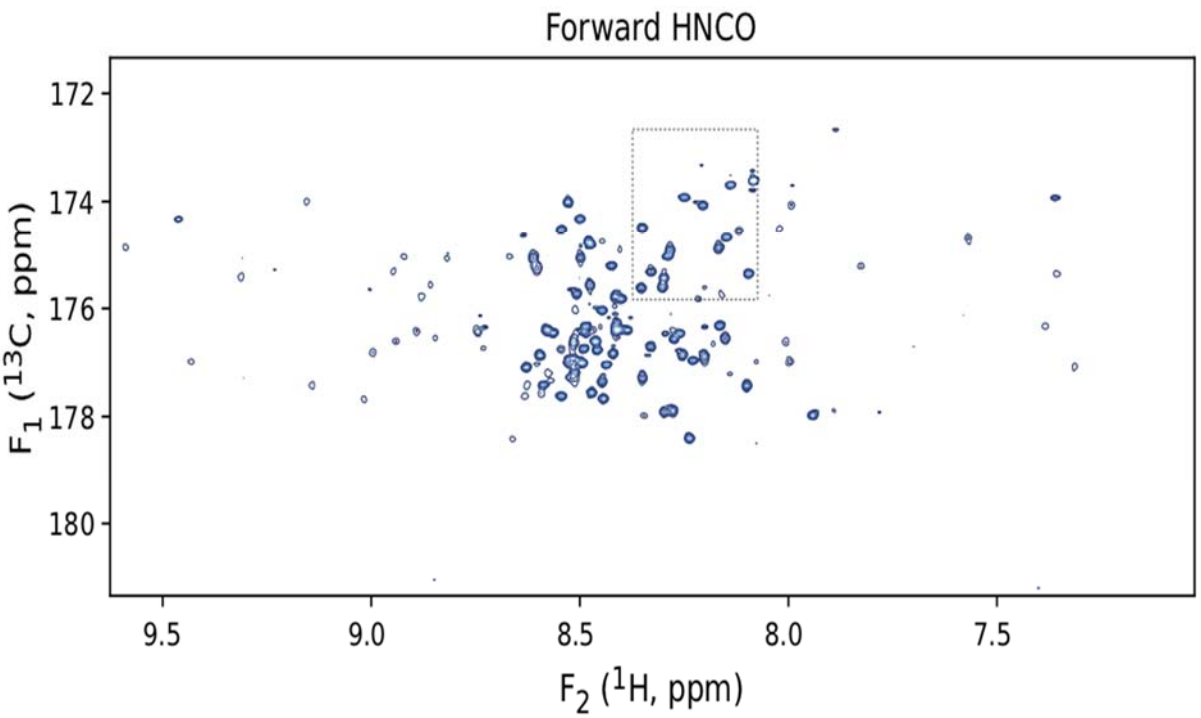

Figure S7. Pressure-jump forward-sampled 2D ^{1}H-^{13}C HNCO spectrum of VA2-ubiquitin, with the boxed region shown in Figure 3, main text

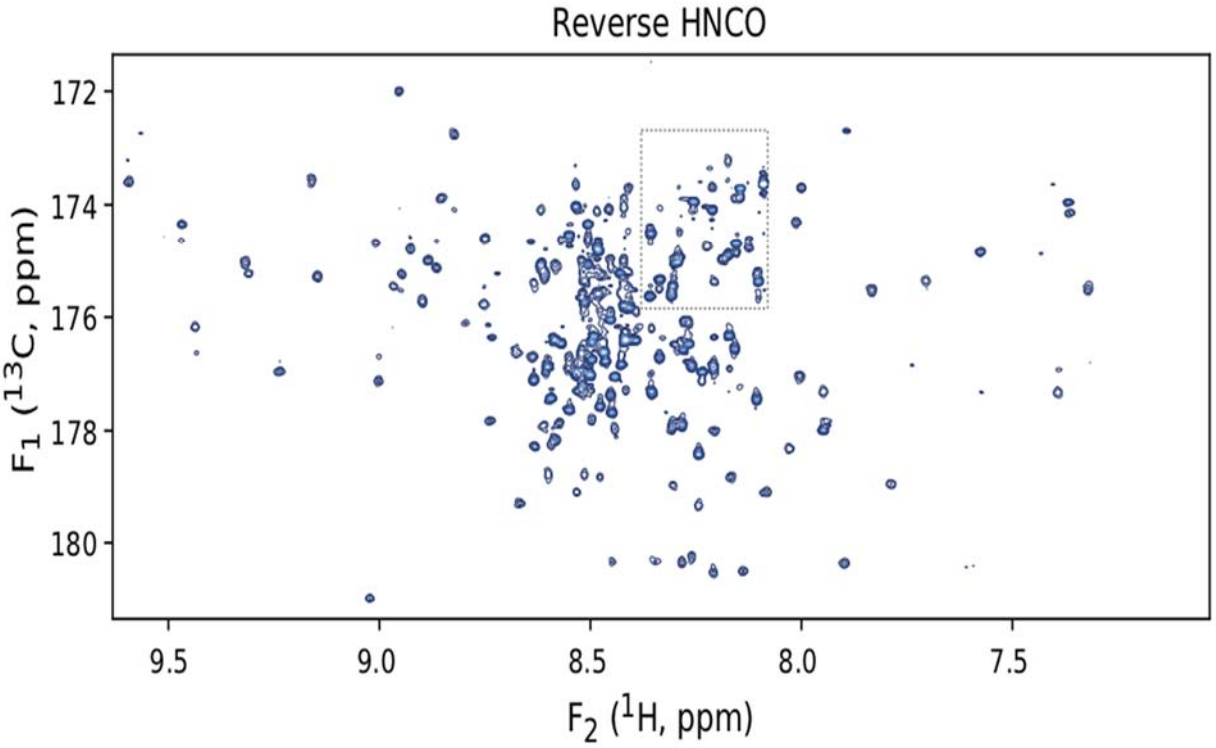

Figure S8. Pressure-jump reverse-sampled 2D ^{1}H-^{13}C HNCO spectrum of VA2-ubiquitin, with the boxed region shown in Figure 3, main text. Peak positions of the I-state correspond to those of Table S1.

Table S1. Intermediate chemical shifts of VA2-ubiquitin at 1 bar.

Res	^{13}C'(I)	^{15}N(I)	^{1}H(U)	^{1}H(F)
M1				
Q2	174.12			8.89
I3	174.10	121.40	8.48	8.49
F4	175.06	125.28	8.63	8.82
V5	174.58	123.91	8.30	9.31
K6	176.70	128.37	8.51	8.93
T7	177.01		8.43	9.00
L8	178.96	120.43	8.61	9.23
T9	175.57		8.29	7.78
G10	174.11	109.21	8.43	7.83
K11	175.73	121.35	8.25	7.35
T12	174.64	120.47	8.49	8.89
I13	174.65	126.57	8.50	9.47
T14	173.79	118.82	8.48	8.87
L15	174.99		8.55	9.16
E16	175.86		8.54	8.17
A17	175.09		8.41	8.89
E18	174.84	119.58	8.52	8.58
P19	175.40			
S20	174.63	103.87	8.63	7.31
D21	176.33	123.43	8.54	8.11
T22	176.64		8.26	8.26
I23		121.10	8.30	8.68
E24	179.09		8.61	
N25	178.00	121.36	8.53	8.08
A26	179.26	123.21	8.31	8.19
K27	180.52	116.40	8.25	8.65
A28	180.30	124.00	8.21	8.13
K29	180.30	119.83	8.28	7.90
I30	178.26	121.08	8.26	8.35
Q31	178.72		8.59	8.58
D32	177.31	119.79	8.52	8.17
K33	177.21	115.26	8.41	7.54
E34	177.95	114.38	8.49	8.73
G35	173.88	108.83	8.44	8.61
I36			8.15	6.45
P37				
P38	178.28			
D39	177.13	113.55	8.59	8.63
Q40	175.51	116.82	8.22	8.00
Q41	176.12	118.00	8.33	7.69
R42	173.89	123.00	8.28	8.77
L43	175.23	124.19	8.15	8.85
I44	175.47	123.24	8.10	9.14
F45	174.43	127.54	8.41	8.75
A46	177.31	132.99	8.36	9.02
G47	174.27	102.36	7.95	8.36
K48	174.62	121.87	8.21	7.99
Q49	175.92	123.88	8.57	8.75
L50	176.73	126.26	8.45	8.52
E51	175.20	122.70	8.56	8.64
D52			8.46	8.42
G53	174.84	109.74	8.49	
R54	175.54	119.04	8.14	7.56
T55	176.57	109.45	8.47	8.94
L56	180.47	120.01	8.50	8.50
S57	177.01	112.84	8.44	9.01
D58	176.93	122.54	8.36	8.02
Y59	174.75	116.17	8.17	7.39
N60	175.67	116.60	8.40	8.22
I61	174.32	120.09	8.10	7.34
Q62	175.90	120.22	8.45	7.99
K63	176.65		8.39	8.48
E64	177.16	118.04	8.50	9.44
S65	174.07	115.65	8.52	8.19
T66	173.22	114.27	8.33	8.95
L67	174.32	123.13	8.17	9.59
H68	174.49	122.92	8.52	9.30
L69	176.19	121.56	8.29	8.39
V70	175.14	122.17	8.36	8.97
L71	175.13	126.91	8.42	8.44
R72	174.10	126.31	8.44	8.58
L73	178.83	120.26	8.42	8.51
R74	176.91	123.08	8.47	8.60
G75	173.64	111.35	8.46	8.55
G76			8.09	8.09

References

1. Piotto, M.; Saudek, V.; Sklenar, V., Gradient-Tailored Excitation for Single-Quantum Nmr-Spectroscopy of Aqueous-Solutions. *J. Biomol. NMR* **1992,** *2* (6), 661-665.
2. Levitt, M. H.; Freeman, R., Compensation for pulse imperfections in NMR spin-echo experiments. *J. Magn. Reson.* **1981,** *43* (1), 65-80.
3. Charlier, C.; Courtney, J. M.; Alderson, T. R.; Anfinrud, P.; Bax, A., Monitoring N-15 Chemical Shifts During Protein Folding by Pressure-Jump NMR. *J. Am. Chem. Soc.* **2018,** *140* (26), 8096-8099.
4. Helgstrand, M.; Hard, T.; Allard, P., Simulations of NMR pulse sequences during equilibrium and non-equilibrium chemical exchange. *J. Biomol. NMR* **2000,** *18* (1), 49-63.